

To be submitted to  
Nuclear Physics

COMITATO NAZIONALE PER L'ENERGIA NUCLEARE  
Laboratori Nazionali di Frascati

LNF-75/53(R)

18 Novembre 1975

J. Banaigs, J. Berger, M. Cottureau, F.L. Fabbri, L. Goldzahl,  
C. LeBrun, P. Picozza and L. Vu-Hai: PRODUCTION OF I=0  
MESONIC STATES IN THE REACTION  $d+d \rightarrow He^4 + X$ .

J. Banaigs<sup>(o)</sup>, J. Berger<sup>(o)</sup>, M. Cottureau<sup>(+)</sup>, F.L. Fabbri, L. Goldzahl<sup>(o)</sup>,  
C. Le Brun<sup>(+)(x)</sup>, P. Picozza and L. Vu-Hai<sup>(+)</sup>: PRODUCTION OF I=0 MESONIC STATES IN THE REACTION  $d+d \rightarrow He^4 + X$ . -

ABSTRACT. -

The inclusive reaction  $d+d \rightarrow He^4 + X$  provides an interesting means of studying I=0 meson systems since, in it, the X system is produced in a pure isoscalar state, with simultaneous formation of a single charged particle. This study deals with missing masses in the range 270 to 1000 MeV/c<sup>2</sup>. Of all the I=0 meson resonances, only the controversial  $\epsilon^0$  can be produced in the S wave; the others can be produced only in odd waves. No signal is obtained for the  $\epsilon^0$ , and the  $\omega^0$  is obtained with only a very weak cross section,  $\sim 1$  nb/sr.

On the other hand, the ABC effect associated with pion production in reactions involving light nuclei is abundantly produced, and accounts for nearly all alpha production in the reaction. This production varies greatly as a function of energy.

---

(o) - CNRS - Département Saturne - France

(+) - Université de Caen - France.

(x) - Thesis to be published.

## 1. - INTRODUCTION. -

In the reaction



whose study will be presented here, because the deuteron and the alpha have isospin zero, the missing mass X is created in a pure  $I=0$  isospin state, and as a result cannot consist of an odd number of  $\pi^0$ s. This very interesting property lets us use the reaction (1) to study the production of  $I=0$  resonances in a pure isospin channel, and also to look for possible violation of isospin conservation in the forbidden reaction  $d+d \rightarrow \text{He}^4 + \pi^0$ .

Different studies of the reaction  $d+d \rightarrow \text{He}^4 + \pi^0$  (1,2) have given no evidence of violation of isospin conservation. Our previous experiment (2) carried out at Saclay with the arrangement described below, and deuterons at 1.89 GeV/c, gave  $d\sigma/d\Omega^X < 1.9 \times 10^{-35} \text{ cm}^2/\text{sr}$  as an upper limit for the pion production cross section at  $\theta^X = 79^\circ$ . The set of results on this reaction provides one of the best indications of the validity of isospin conservation.

Two bubble chamber experiments, one at 3.0 GeV/c (3), the other at 7.9 GeV/c (4), have studied the production of mesons in  $d+d$  interactions; in these, single alpha production could not be observed, but each gave some  $d+d \rightarrow d+d + \pi^+ + \pi^-$  events where the isospin selection rules are the same. The inclusive spectrum obtained at Birmingham (5) with deuterons at 1.69 GeV/c in the reaction  $d+d \rightarrow \text{He}^4 + X$  did not give evidence of the sought-after ABC effect. Finally, an experiment with poor statistics that was carried out on Saturne at 3.8 GeV/c with another spectrometer gave evidence of weak production of  $\omega^0$ .

The aim of the experiment described here was to study the inclusive production of  $I=0$  resonances of mass less than  $1000 \text{ MeV}/c^2$  - the maximum missing mass for incident deuterons at 3.8 GeV/c - in favourable experimental conditions, for the reason that these resonances are associated with only one charged particle, and to look for possible production of the ABC effect in a reaction involving four nucleons, and to study its angular and energetic characteristics.

## 2. - DESCRIPTION OF THE EXPERIMENT. -

## 2.1. - Experimental arrangement. -

Previous studies (3,5) had shown that very weak alpha production

cross sections ( $\leq 1 \mu\text{b}$ ) must be expected when the total  $d+d$  cross section measured at  $3 \text{ GeV}/c$ <sup>(3)</sup> is  $120 \text{ mb}$ . We had therefore to use an arrangement that was capable both of taking the most intense incident flux that Saturne could produce ( $2 \times 10^{11}$  deuterons per burst of 400 ms) and of selecting alphas from among other particles produced in the target. The ratio of the number of alphas to the total number of particles produced could reach  $10^{-5}$  in the most unfavourable cases. The double analysing magnetic spectrometer used for the study of the reaction  $d+p \rightarrow \text{He}^3 + X$ , and described in<sup>(7)</sup>, met these requirements quite adequately after some modifications.

The arrangement used is shown in Fig. 1. The position and form of the incident beam were permanently controlled by three wire chambers. At the target, the beam had a marked Gaussian profile in the two planes with a full width of 15 mm at half maximum along the vertical axis, and varying from 12 to 24 mm in the horizontal plane as the incident momentum of the deuterons varied from 3.8 to 1.9  $\text{GeV}/c$ . Relative monitoring of the number of incident deuterons was ensured by two scintillation counter telescopes; the first,  $m_0$ , viewed a 2 mm plastic target placed in the beam and with a response independent of the angle in which the spectrometer was working; the second,  $m_1$ , counted particles emitted at  $70^\circ$  from the target. The count ratio of these two monitors remained constant to within  $\pm 1\%$ .

The liquid deuterium was contained in a stainless steel cylinder 5.9 cm long and 8 cm in diameter whose entry and exit windows were each  $50 \mu$  thick. The vacuum chamber containing the target had titanium windows  $50 \mu$  thick on the trajectory of the beam. The target-empty contribution was reduced by having boxes filled with hydrogen gas with very thin windows ( $10 \mu$  mylar) placed upstream and downstream of the target. The spectrometer used was double analysing, dispersing at the intermediate image and achromatic at the final image. The whole spectrometer, including the intermediate image counters, was in a vacuum. At the intermediate image, particle detection was ensured by having a set of five contiguous scintillation counters ( $I_1$  to  $I_5$ ) each made up of a scintillator  $7 \times 1 \times 0.1 \text{ cm}^3$  connected to a PS 2010 photomultiplier. In order to have good amplitude discrimination, the final image detection system was made up of three successive scintillation counters  $F_1, F_2, F_3$  ( $8 \times 6 \times 0.4 \text{ cm}^3$ ).

## 2.2. - Experimental method. -

### 2.2.1. - Kinematics. -

In an inclusive reaction of the type  $1+2 \rightarrow 3+X$  where 3 is the detected particle, the invariant mass of the system X is a function of the two variables  $P_3$  and  $\theta_3$  defined by the spectrometer:

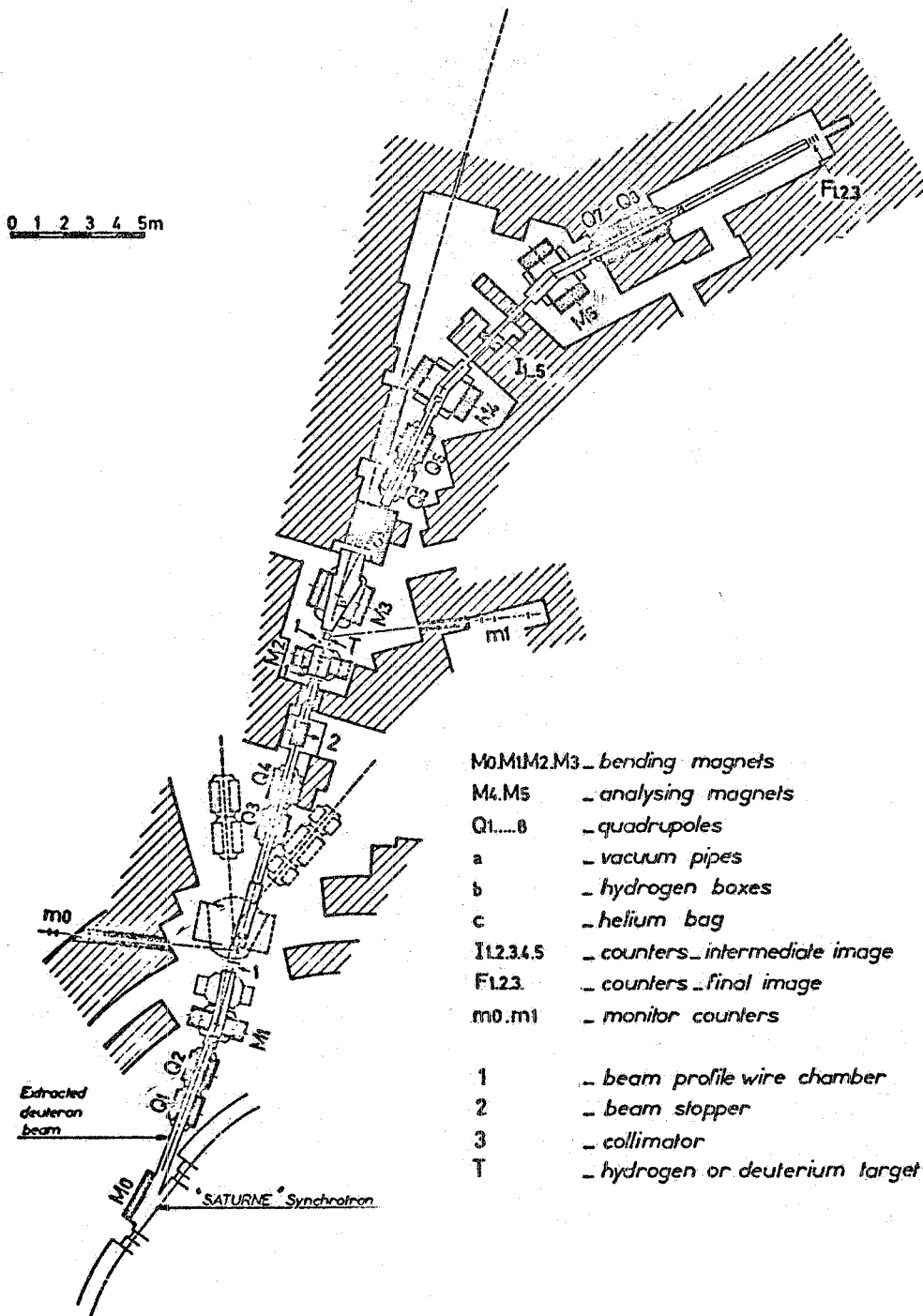


FIG. 1 - Experimental arrangement.

$$M_X^2 = (W - E_3)^2 - (\vec{P}_1 - \vec{P}_3)^2 = m_1^2 + m_2^2 + m_3^2 + 2E_1 m_2 - 2E_3(m_2 + E_1) + 2P_1 P_3 \cos\theta_3$$

In our particular case, 3 is a heavy particle whose velocity in the centre of mass system is less than the velocity of the centre of mass in the laboratory system. This results in a limiting value for the alpha emission angle  $\theta_3$  in the laboratory. Figure 2 shows the variation of this angle as a function of the momentum of the alpha for different values of  $M_X$ , and for deuterons at 2.5 GeV/c, as the angle in the centre of mass varies between 0 and  $180^\circ$ . We see that the magnetic rigidity of the alphas,

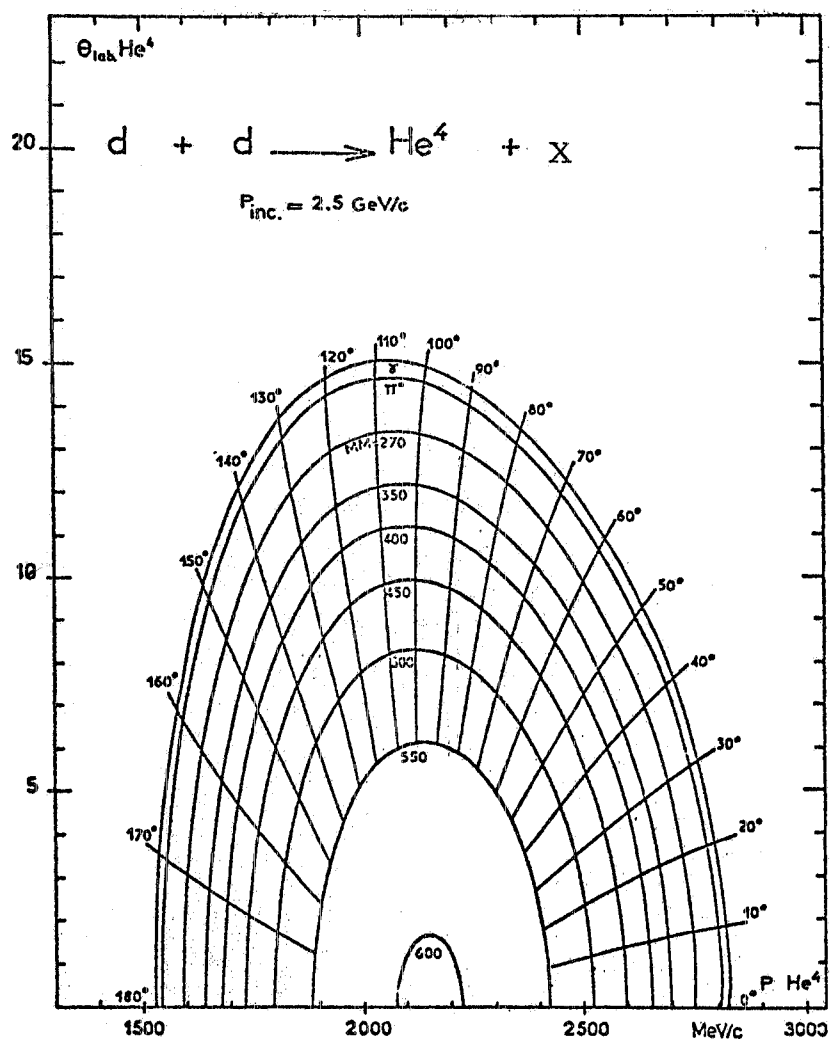


FIG. 2 - Kinematics of the reaction  $d+d \rightarrow \text{He}^4 + X$  at  $P_1 = 2.5 \text{ GeV/c}$ . Laboratory angle versus the alpha momentum: curves at constant missing mass, and for constant centre of mass angle.

$P/z$ , is always far from the momentum of the incident deuterons but that, on the other hand, the  $P/z$  corresponding to the alphas emitted in the forward direction in the centre of mass is about half this incident momentum. For this momentum region, and for angles  $\theta_3$  less than  $6^\circ$ , the flux of protons produced by stripping deuterons is such that the number of particles found in the spectrometer is much greater than is compatible with correctly functioning electronics, and so any measurement becomes impossible. Notice, however, that since the reaction is symmetric, we are not prevented from obtaining a complete angular distribution in the centre of mass.

### 2.2.2. - The spectrometer. -

The currents in the seven magnets and quadrupoles making up the spectrometer were calculated for alphas produced at the centre of the target, with given momentum, and which crossed the central intermediate image counter. Energy losses in the target and the various absorbing media were taken into account. The dispersion coefficient  $(\Delta P/P)\Delta X$  at the intermediate image allows the calculation of the central momentum in the other counters: it was 0.97% per cm. The momentum analysed by the spectrometer is known with a precision of 0.5%<sup>(7)</sup>. The geometric aperture defined by the square collimator 3, which measured  $8 \times 8 \text{ cm}^2$ , was  $\pm 7.3 \text{ mrad}$  in the two planes.

The acceptance of the spectrometer was calculated with a Monte Carlo program, taking into account energy loss and multiple scattering in each of the materials crossed, and also the dimensions of the incident beam. Fig. 3 shows the variation of the reduced acceptance  $\Delta P_3 \Delta \Omega_3 / P_3$  of the central intermediate image counter as a function of the momentum

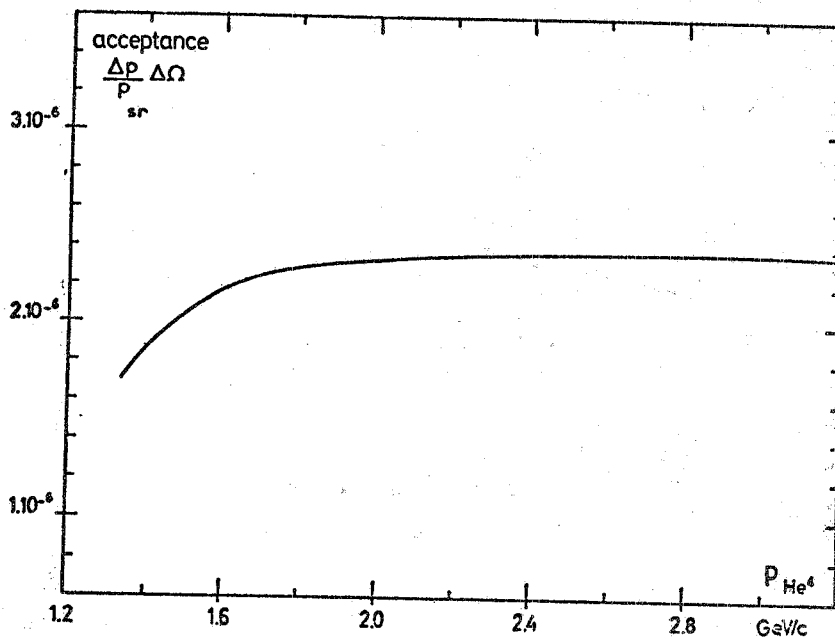


FIG. 3 - Spectrometer acceptance as a function of the momentum analysed of alpha particles.

analysed. The resolution is calculated with the same program, by looking at the transmission of particles created in the target at given momenta. It was  $\pm 0.65\%$  and varied slightly with the dimensions of the incident beam. In each of the analysing magnets  $M_4$  and  $M_5$ , the values of the magnetic field was permanently controlled with better precision than  $10^{-4}$  by using magnetic nuclear resonance probes. The exact value of the detection angles  $\theta_3$  had been determined earlier by means of a 2-body reaction  $d + p \rightarrow \text{He}^3 + \pi^0$  (7, 8).

### 2.2.3. - Identification of particles. -

The 14 m distance between the two groups of counters allowed easy separation of the deuterons and alphas, which have the same time of flight, from the other particles. To select the alphas we used a pulse-height discrimination on the four counters ( $I_i, F_1, F_2, F_3$ ) crossed by particles. Because of their double charge, alphas lose on average four times more energy in matter than do deuterons with the same  $P/z$ . Threshold curves and pulse-height spectra were recorded at different momenta. Fig. 4 shows an example of these curves; it can be seen that the alphas are very well separated from the deuterons; maximum deuteron contamination was always less than 1% of the number of alphas counted.

The electronics logic diagram is shown in Fig. 5. The thresholds of channel A were set to accept particles with ionisation greater than or equal to that of the deuterons. This channel was used for a control count and for adjustment, at each momentum of the spectrometer, of the high voltages applied to the photomultipliers.

The alphas were counted in two ways, B and B', starting from discriminators that define the separation of deuterons and alphas. B is composed of coincidence circuits of variable resolution, and B' of a time-amplitude convertor with an analogue-digital coder which allowed recording of time of flight spectra of the particles in the five channels simultaneously. The rate of random events in the coincidences and corrections due to dead time in the time of flight system were always less than 1%, and often as low as 0.1%.

## 3. - DATA ANALYSIS AND RESULTS. -

### 3.1. - Acceptance corrections and losses due to nuclear interactions. -

The currents in the magnets and quadrupoles of the spectrometer were optimised for the momentum band analysed by the central intermediate image counter, and the acceptance  $\Delta P_3 \Delta \Omega_3$  was calculated by this same



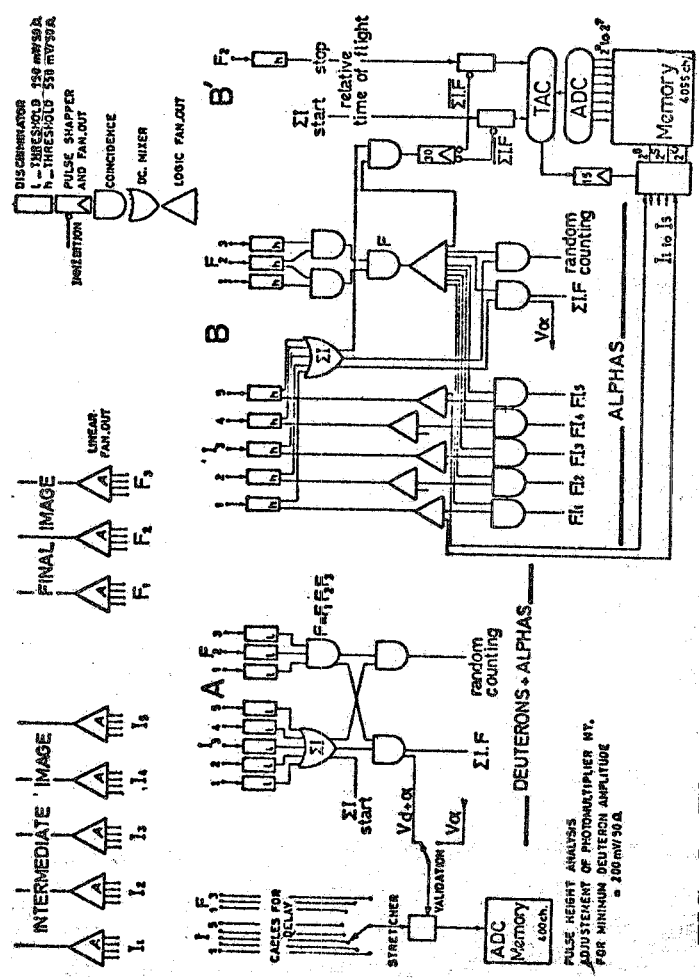
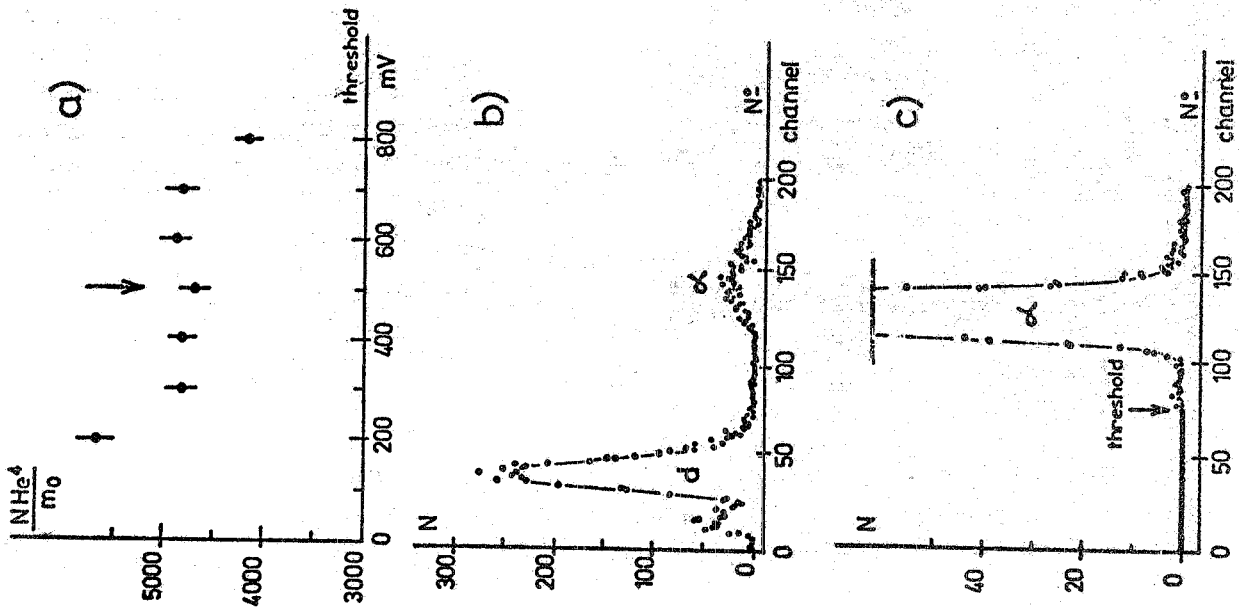


FIG. 5 - Electronics logic diagram.

FIG. 4 - a) Threshold curves from the I counters, the F counters being placed at a threshold of 550 mV; b) amplitude spectrum from the I<sub>1</sub> counter (thickness 1 mm) obtained at P/z = 1 GeV/c on a target of <sup>12</sup>C; c) typical amplitude spectrum from the F<sub>2</sub> counter, checked by the coincidence (I<sub>1</sub> F<sub>1</sub> F<sub>2</sub> F<sub>3</sub>), recorded during measurement at P/z = 1003.4 MeV/c,  $\theta_{lab} = 7.4^\circ$ . The whole peak comprises 10786 alphas, to the right of it one can see that deuteron contamination is negligible.

counter. Counts from the four lateral counters covering the adjacent momentum bands had then to be corrected to take into account losses due to the slight optimisation failure of the spectrometer with corresponding momenta, and the fact that these counters were not on the focus, so their acceptance was weaker than that of the central one. Correction coefficients to be applied to each alpha count in the lateral channels were determined experimentally with good statistical accuracy by recording deuterons produced at the same time as alphas in the reaction  $d+d \rightarrow d+X$ , and taking the ratios of the counts from each of the lateral channels to the count from the central one for the same momentum.

We checked that the coefficients determined in this way were identical for alphas and deuterons.

Count losses due to alpha-nuclear interactions in the various materials encountered in the spectrometer were calculated by assuming an  $\text{He}^4$ -nucleus cross section to be the product of the total cross section of the  $\text{He}^4$ -nucleon<sup>(9)</sup> and the geometric factor  $A^{2/3}$  of each absorbent nucleus of mass number A. These losses decreased from 20 to 8% when the magnetic rigidity of the alphas was increasing from 700 to 1300 MeV/c.

### 3.2. - Calculation of cross sections. -

The differential cross sections were obtained from the usual formula

$$\frac{d^2 \sigma}{dp_3 d\Omega_3} = \frac{\alpha_{cp} - \alpha_{cv}}{\rho D_x \ell s},$$

where  $\alpha_{cp}$  and  $\alpha_{cv}$  represent respectively the corrected number of alphas created with the target full or empty for x events on the monitor.  $D_x$  is the number of incident deuterons corresponding to x; its value was obtained from the activity of a sample of carbon irradiated by the beam. For the activation cross sections of the deuteron activated  $^{12}\text{C}$ , we took values deduced from the value obtained at 3.76 GeV/c<sup>(10)</sup>, and assumed that the cross sections of the activation reactions  $^{12}\text{C}(d, pnn)^{11}\text{C}$  and  $^{12}\text{C}(p, pn)^{11}\text{C}$  behave similarly as a function of energy. The factors  $\rho$ ,  $s$ , and  $\ell$  represent respectively the nuclear density of the deuterons in the target, the spectrometer acceptance at the momentum analysed by the central counter, and the thickness of the target.

After verifying that the target-empty contribution varied monotonically with the momentum analysed, we measured it for only some values of  $P_3$  on each spectrum, and determined the missing values from a polynomial fit. The contribution of the target-empty to the total observed count varied between 8 and 30% for different cases.

The error associated with each experimental point on the spectra

takes into account only the statistical error on the subtraction  $a_{cp} - a_{cv}$ . Error in the measurement of the number of incident deuterons was of the order of  $\pm 10\%$ . It affects neither the shape of the spectra, nor the angular distribution at a given energy, and so is not given in the results. On the other hand, it has been included in the production curves as a function of energy. With errors from acceptance calculations plus various corrections, we arrive at a possible systematic error of 15% for these curves.

Table I summarises the experimental conditions in which the spectra shown in Figs. 6-18 were obtained. On these figures a supplementary scale gives the missing mass value associated with the momentum of the  $\text{He}^4$ . A glance at these spectra shows that the production is strongly dependent on the energy, since the maximum of the differential cross section in the laboratory goes from  $200 \mu\text{b}/(\text{sr. GeV}/c)$  at  $1.89 \text{ GeV}/c$  to  $1.5 \mu\text{b}/(\text{sr. GeV}/c)$  at  $3.82 \text{ GeV}/c$ .

For the analysis of the spectra we shall separate the study into two parts: one dealing with masses of less than  $500 \text{ MeV}/c^2$  that appear strongly related to the ABC effect; the other with  $I=0$  isospin meson states of masses lying between  $500$  and  $1000 \text{ MeV}/c^2$ .

TABLE I

Characteristics of the spectra obtained.

| $P_1$<br>GeV/c | $\theta_3$<br>Degrees | $W^x$<br>GeV/c <sup>2</sup> | $M_{\text{max}}$<br>GeV/c <sup>2</sup> | Position of the top<br>of the first peak<br>MeV/c <sup>2</sup> <sub>2</sub> | N <sup>o</sup> Fig. |
|----------------|-----------------------|-----------------------------|--|---|---------------------|
| 1.89           | 0.3                   | 4.126                       | 0.399                                  | 302.0 $\pm$ 7.0   | 6                   |
| 2.10           | 0.3                   | 4.196                       | 0.469                                  | 324.0 $\pm$ 9.0   | 7                   |
| 2.29           | 0.3                   | 4.259                       | 0.532                                  | 326.0 $\pm$ 11.0  | 8                   |
| 2.50           | 0.3                   | 4.331                       | 0.604                                  | 340.0 $\pm$ 13.0  | 9                   |
| 2.50           | 4.5                   | 4.331                       | 0.575                                  | 316.0 $\pm$ 13.0  | 10                  |
| 2.50           | 6.4                   | 4.331                       | 0.544                                  | 312.0 $\pm$ 13.0  | 11                  |
| 2.50           | 7.4                   | 4.331                       | 0.525                                  | 310.0 $\pm$ 12.0  | 12                  |
| 2.50           | 8.3                   | 4.331                       | 0.503                                  | 306.0 $\pm$ 13.0  | 13                  |
| 2.50           | 11.0                  | 4.331                       | 0.412                                  | 318.0 $\pm$ 8.0   | 14                  |
| 2.70           | 0.3                   | 4.401                       | 0.674                                  | 342.0 $\pm$ 16.0  | 15                  |
| 3.32           | 0.3                   | 4.619                       | 0.892                                  | 352.0 $\pm$ 23.0  | 16                  |
| 3.66           | 0.3                   | 4.740                       | 1.013                                  | -   | 17                  |
| 3.82           | 0.3                   | 4.796                       | 1.069                                  | -   | 18                  |

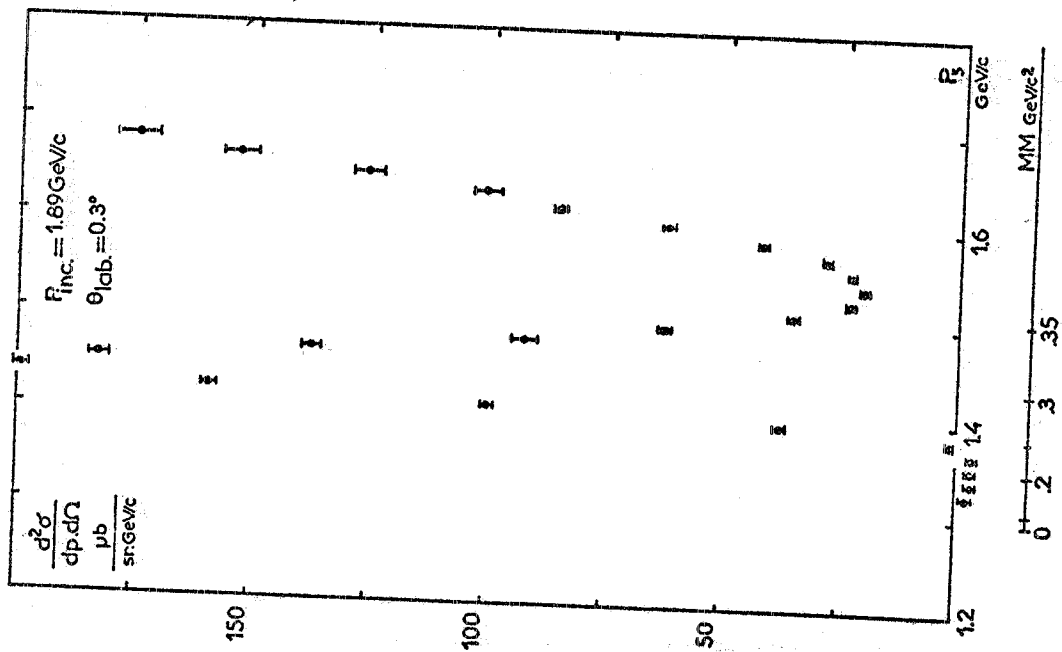


FIG. 6 - Momentum spectrum of alphas produced at  $0.3^\circ$  by deuterons at  $1.89 \text{ GeV/c}$

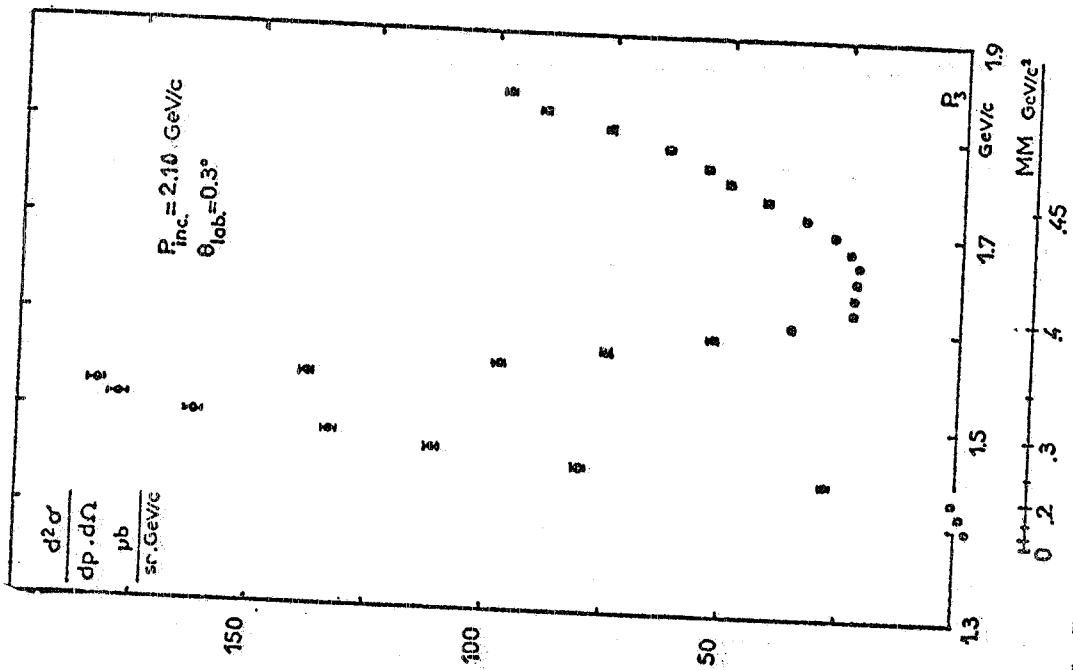


FIG. 7 - Momentum spectrum of alphas produced at  $0.3^\circ$  by deuterons at  $2.10 \text{ GeV/c}$

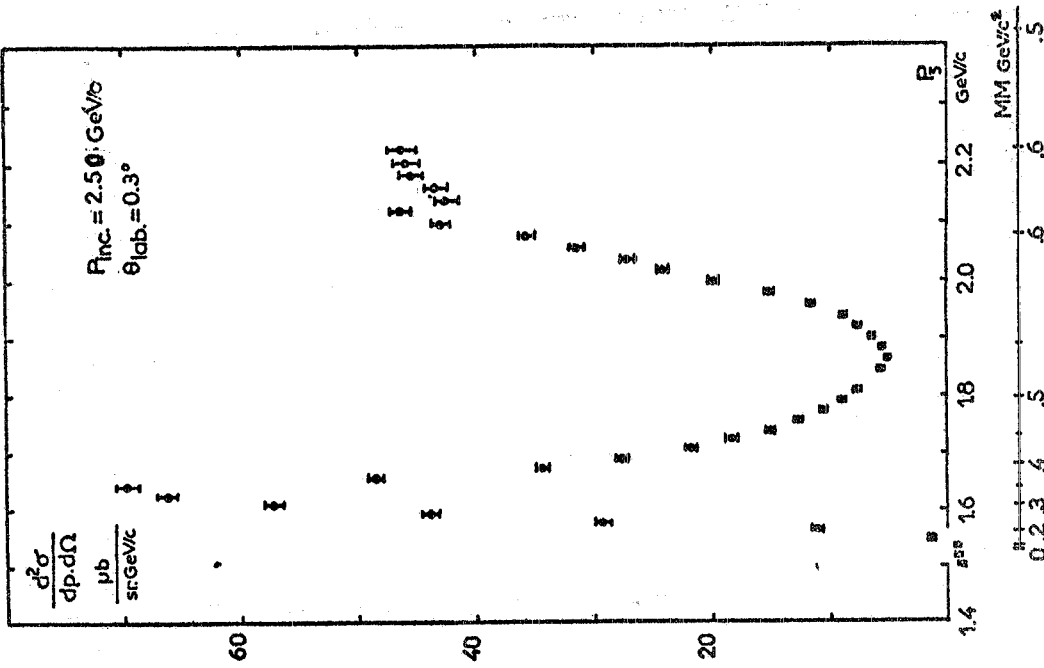


FIG. 9 - Momentum spectrum of alphas produced at  $0.3^\circ$  by deuterons at  $2.50 \text{ GeV}/c$ .

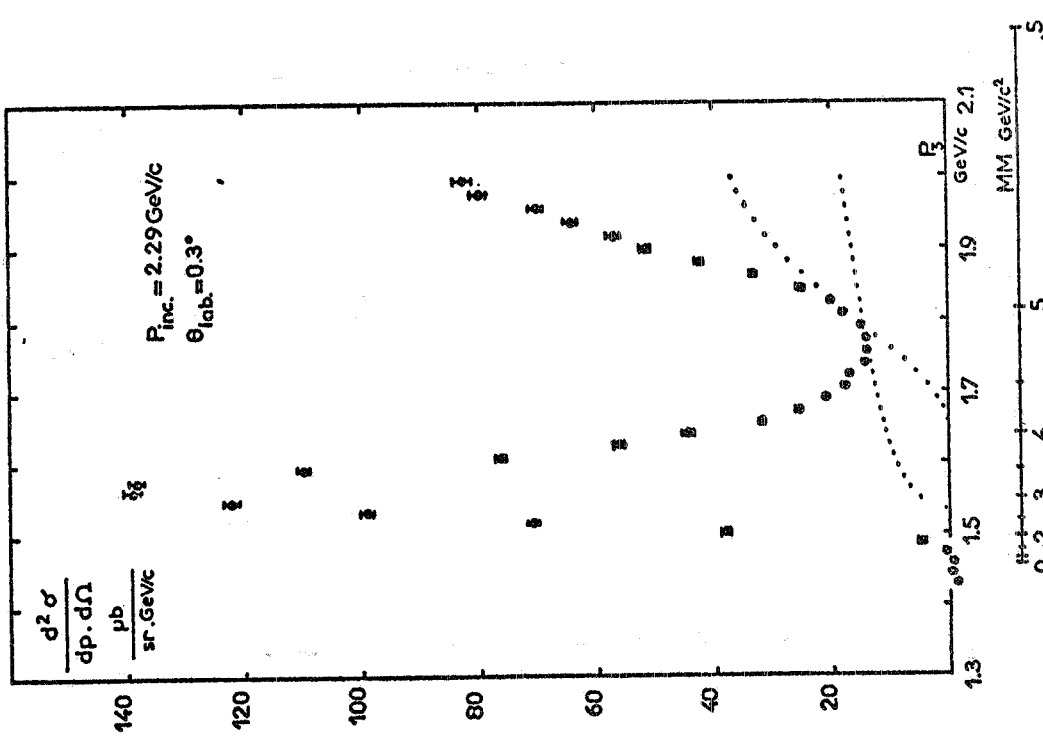


FIG. 8 - Momentum spectrum of alphas produced at  $0.3^\circ$  by deuterons at  $2.29 \text{ GeV}/c$ . The dotted lines represent the statistical phase spaces for  $\alpha + 2\pi$  and  $\alpha + 3\pi$ , arbitrarily normalised.

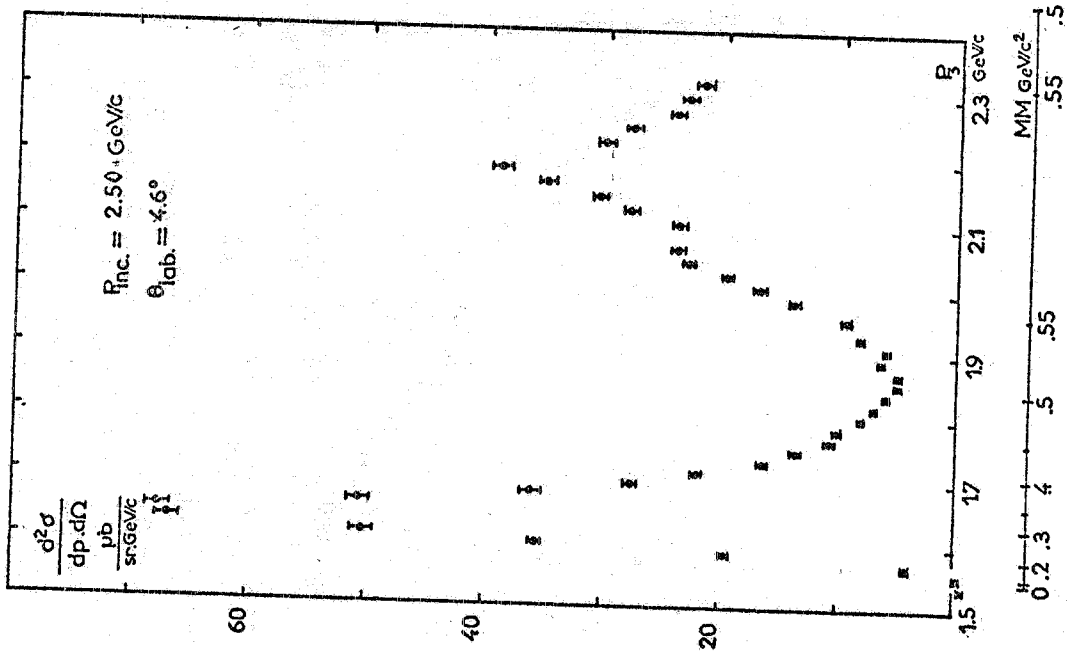


FIG. 10 - Momentum spectrum of alphas produced at  $4.6^\circ$  by deuterons at  $2.50 \text{ GeV/c}$ .

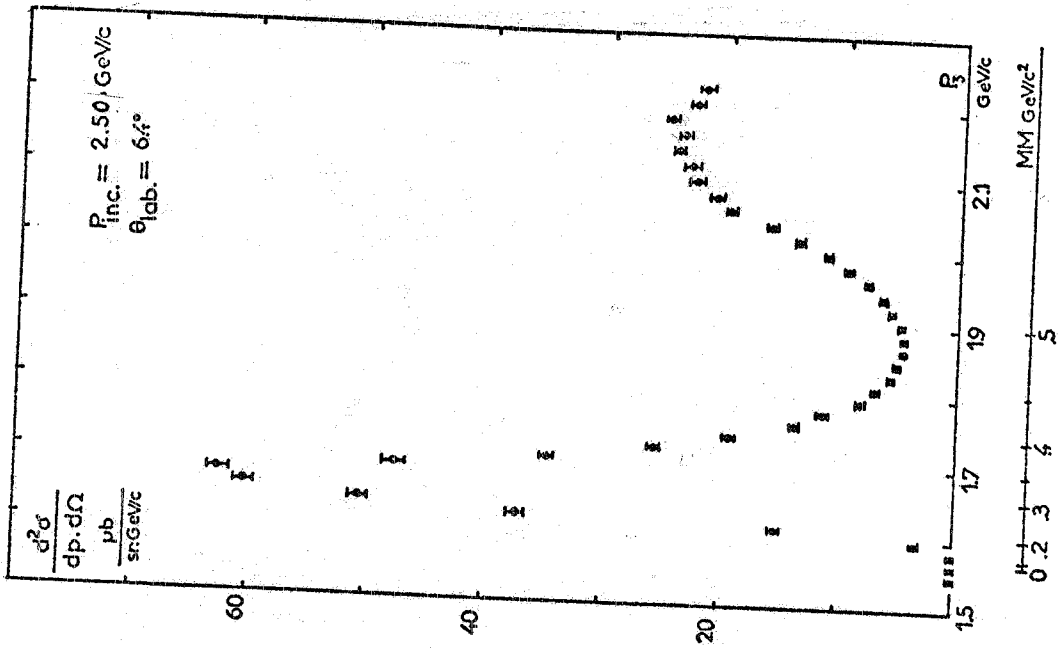


FIG. 11 - Momentum spectrum of alphas produced at  $6.4^\circ$  by deuterons at  $2.50 \text{ GeV/c}$ .

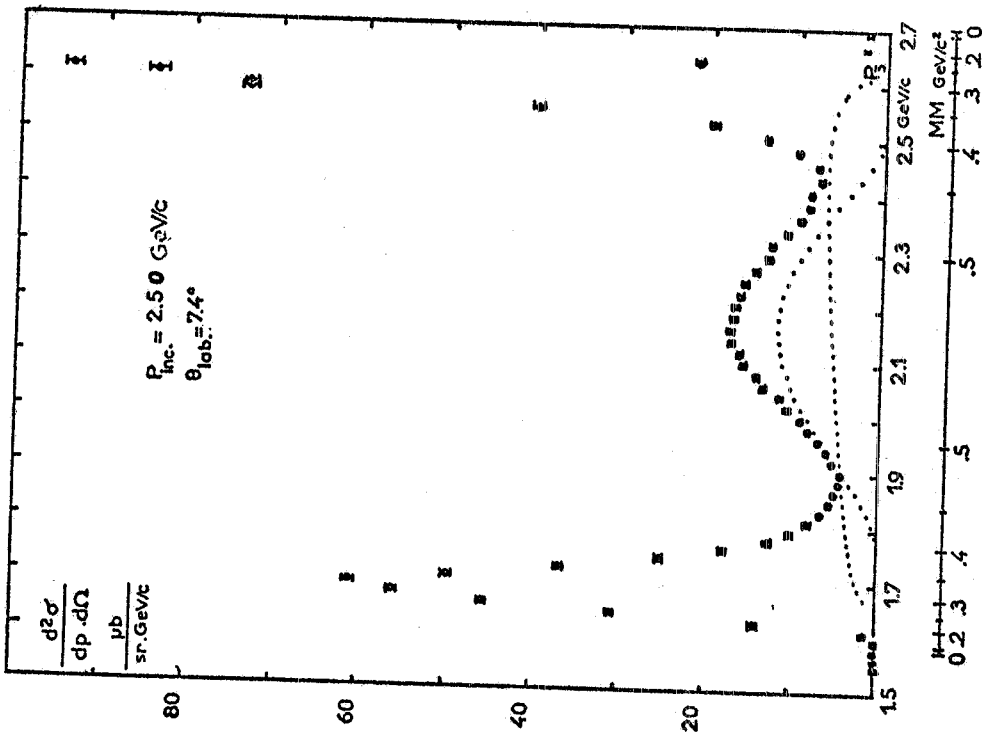


FIG. 12 - Momentum spectrum of alphas produced at  $7.4^\circ$  by deuterons at 2.50 GeV/c. The dotted lines represent the statistical phase spaces for  $\alpha + 2\pi$  and  $\alpha + 3\pi$ , arbitrarily normalised.

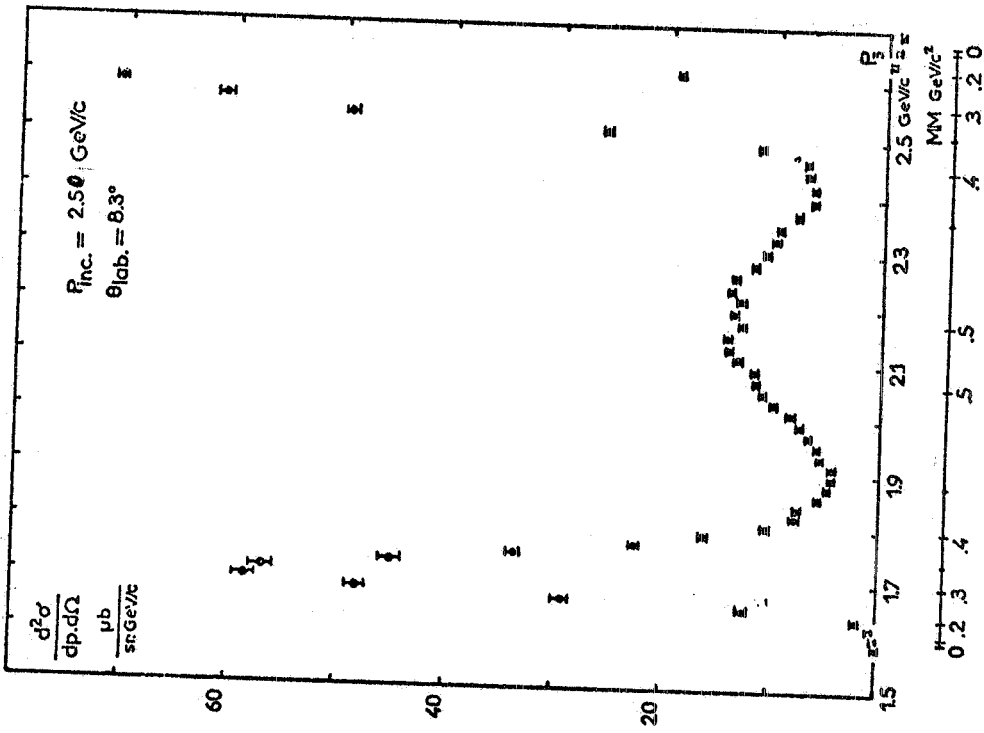


FIG. 13 - Momentum spectrum of alphas produced at  $8.3^\circ$  by deuterons at 2.50 GeV/c.

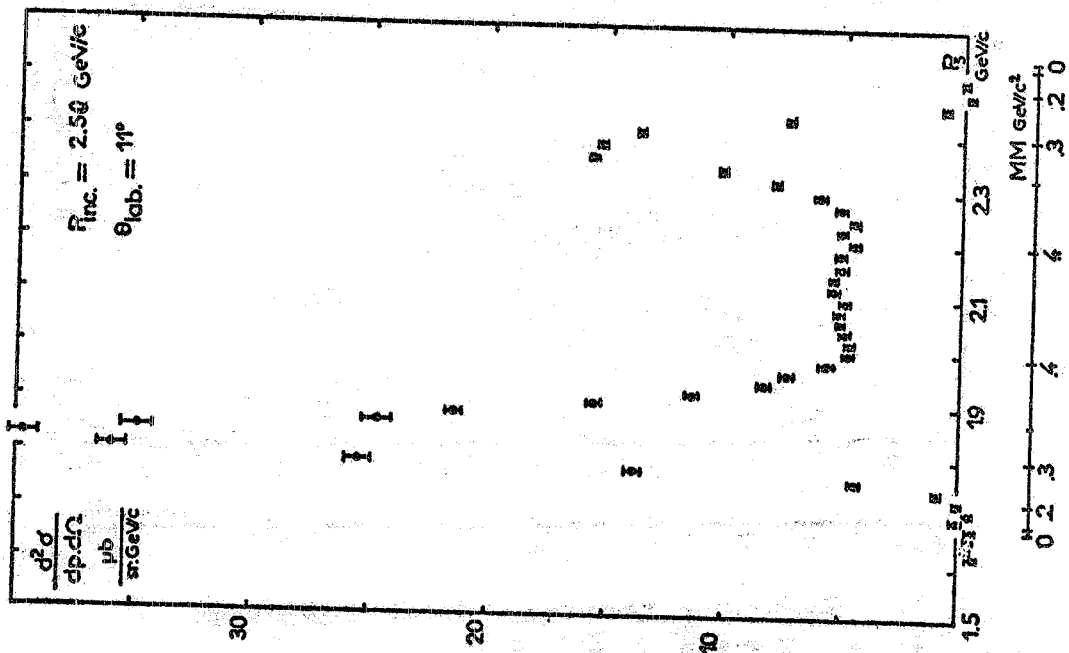


FIG. 14 - Momentum spectrum of alphas produced at  $11.0^\circ$  by deuterons at 2.50 GeV/c.

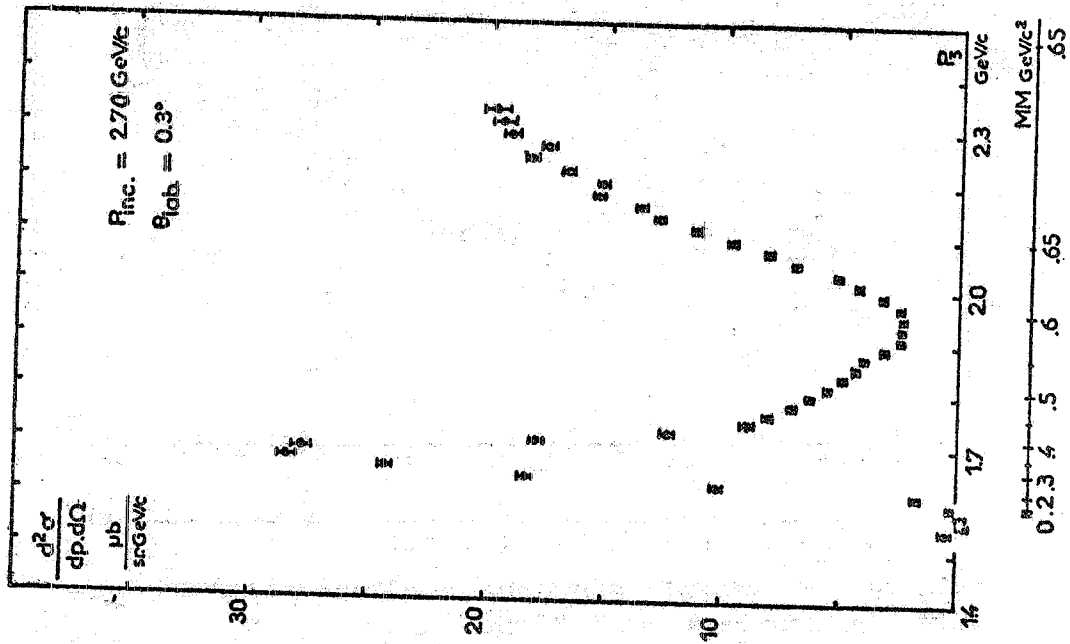


FIG. 15 - Momentum spectrum of alphas produced at  $0.30^\circ$  by deuterons at 2.70 GeV/c.



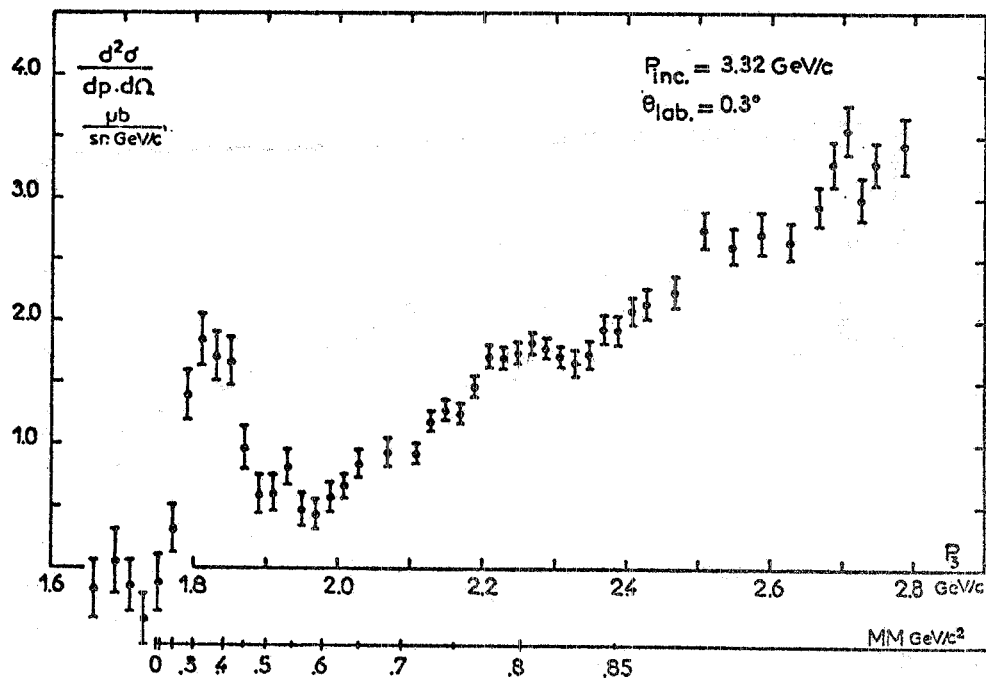


FIG. 16 - Momentum spectrum of alphas produced at  $0.3^\circ$  by deuterons at  $3.32 \text{ GeV}/c$ .

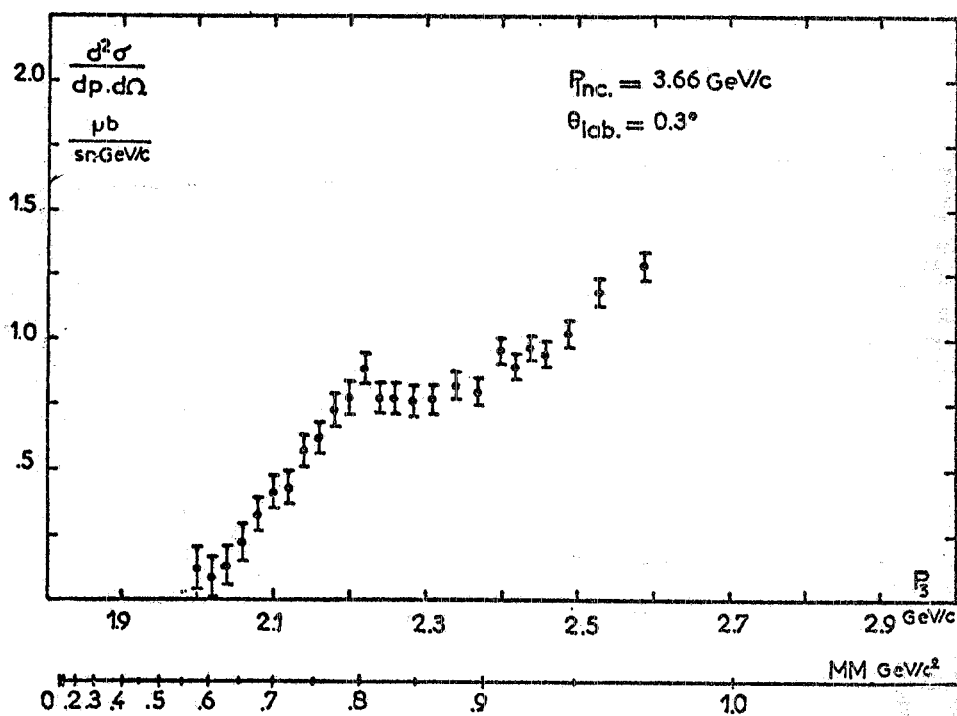


FIG. 17 - Momentum spectrum of alphas produced at  $0.3^\circ$  by deuterons at  $3.66 \text{ GeV}/c$ .

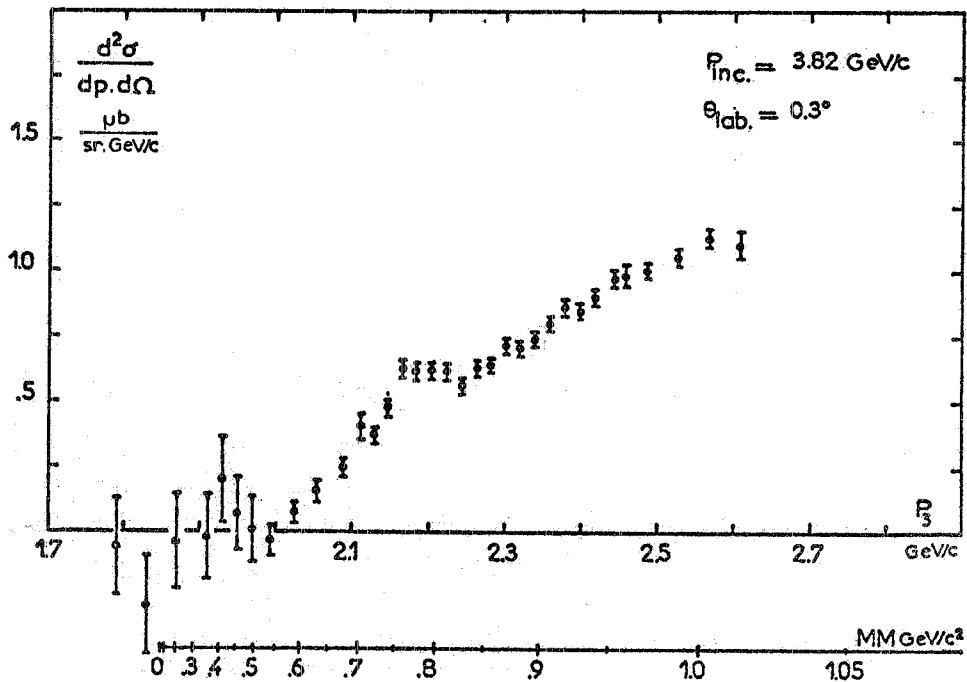


FIG. 18 - Momentum spectrum of alphas produced at  $0.3^\circ$  by deuterons at  $3.82 \text{ GeV}/c$ .

#### 4. - THE ABC AND DEF EFFECTS. -

##### 4.1. - Review of previous results. -

The ABC effect was initially discovered by Abashian, Booth, and Crowe in the reaction  $p+d \rightarrow \text{He}^3 + X$  (11). It is the name given to an important structure observed in the spectra of the inclusive reactions  $p+d \rightarrow d+X$  and  $n+p \rightarrow d+X$  (12, 13);  $p+d \rightarrow \text{He}^3 + X$  (7, 11, 13); and  $d+d \rightarrow \text{He}^4 + X$  (14) near the  $2\pi$  threshold. Such a structure has never been observed in pion-nucleon interactions.

Previous results, especially those obtained from  $d+p \rightarrow \text{He}^3 + X$  (7), have shown that:

- i) the mass position of the ABC effect changes significantly with kinematic conditions;
- ii) the ABC effect shows up mainly in the  $I=0$  isospin state, the spectrum  $d+p \rightarrow \text{He}^3 + X$  ( $I=1$ ) showing only a very small deviation with respect to phase space;
- iii) the production cross section is strongly dependent on the emission angle of the  $\text{He}^3$  and on the total energy of the reaction;

iv) a large structure kinematically linked with the maximum observable missing mass is associated with the ABC effect;

v) most of the spectra show, around 450 MeV/c, a structure called the DEF effect, smaller than the ABC effect, but with the same angular and energetic characteristics.

These results clearly show that the ABC effect is not a resonance but rather a phenomenon linked to production mechanisms.

#### 4.2.- The ABC effect in the reaction $d + d \rightarrow He^4 + X$ .-

All recorded spectra of incident momenta less than 3.32 GeV/c are dominated by important peaks situated at missing masses slightly greater than the mass of the  $2\pi$ ; there is also a large structure near the maximum observable missing mass (Figs. 6-15). At 3.32 GeV/c (see Fig. 16) the first peak still appears near 350 MeV/c<sup>2</sup>, but it has completely disappeared at 3.82 GeV/c (see Fig. 18). At this energy we notice that, within the limit of statistical error, there is no alpha production for missing masses less than 550 MeV/c<sup>2</sup>. In Figs. 8 and 12, the dotted curves represent statistical phase spaces for  $d+d \rightarrow He^4 + 2\pi$  and  $He^4 + 3\pi$  which were calculated taking into account the resolution, and which were arbitrarily normalised. Their shapes are very unlike those of the experimental spectra and in no case can they account for the appearance of the spectra. In particular,  $3\pi$  production alone cannot completely explain the central bump on our spectra. Table I shows that the mass corresponding to the top of the first peak varies with the total energy and the angle. These different characteristics have led us to attribute the structures observed in these spectra to an effect analogous to the ABC effect as observed in  $n+p \rightarrow d+X$  and  $d+p \rightarrow He^3+X$ . We notice that in this reaction the effect is much clearer than in others, the first peak-to-valley ratio lying between 8 and 10, while in the reaction  $d+p \rightarrow He^3+X$  it was only between 2 and 2.5, and of the order of 1 in  $n+p \rightarrow d+X$ .

To determine the variation in alpha production as a function of energy, we integrated the inclusive differential cross sections  $d^2\sigma/d\Omega^*dM$  at  $\theta_{lab} = 0^\circ$ , between the minimum and maximum observable missing mass. We thus obtained the production curve of alphas emitted at  $\theta_{c.m.}^* = 180^\circ$  (or  $0^\circ$  since the reaction is symmetric) as a function of the total energy  $W^*$ , Fig. 19. This operation cannot be applied to spectra obtained at angles  $\theta_{lab}$  different from  $0^\circ$ , since in these conditions the alpha angle  $\theta_{c.m.}^*$  varies with the missing mass. We can see from Fig. 19 that at  $\theta_{c.m.}^* = 180^\circ$ , the alpha production presents an important maximum for  $W^* = 4.24$  GeV ( $P_d = 2.2$  GeV/c). In the reaction  $d+p \rightarrow He^3+X^{(7)}$ , the production for the ABC effect alone was found for  $W^* = 3.38$  GeV ( $P_d = 3.24$  GeV/c). Figure 20 shows the differential cross section  $d\sigma/d\Omega^*$ ,  $\theta_{c.m.}^* = 180^\circ$ , for the two

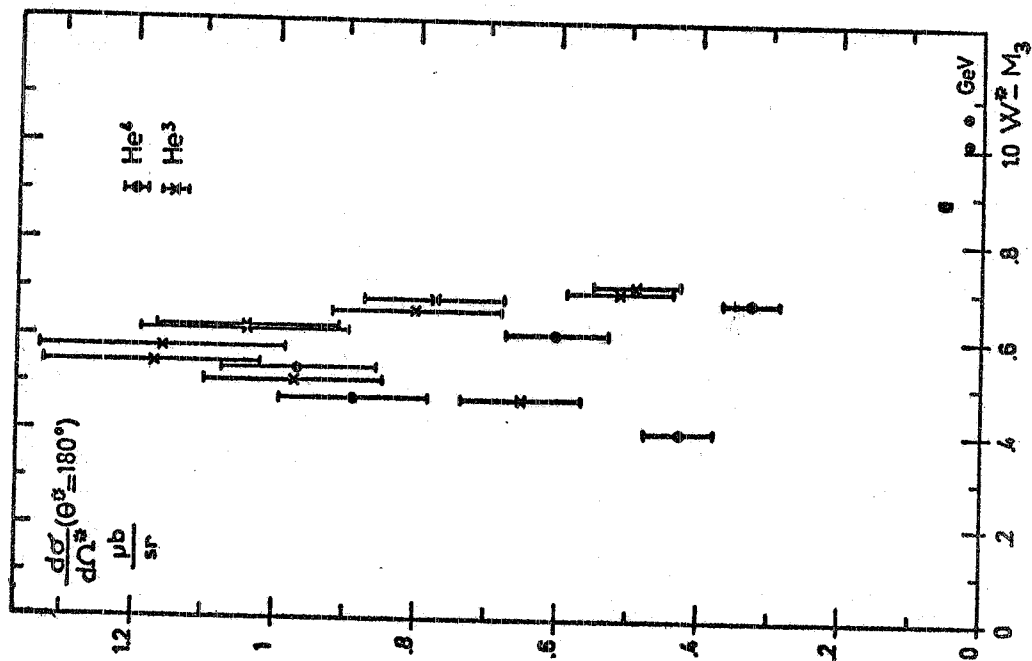


FIG. 20 - Comparison of  $\text{He}^4$  and  $\text{He}^3$  production as a function of  $W^2 - m_3^2$  ( $m_3$  is the mass of the detected nucleus),  $\theta_{\text{c.m.}}^* = 180^\circ$ . Results for  $\text{He}^3$  are taken from ref. (7) by integrating on the missing mass the  $\text{He}^3$  production between the minimum and the maximum missing mass.

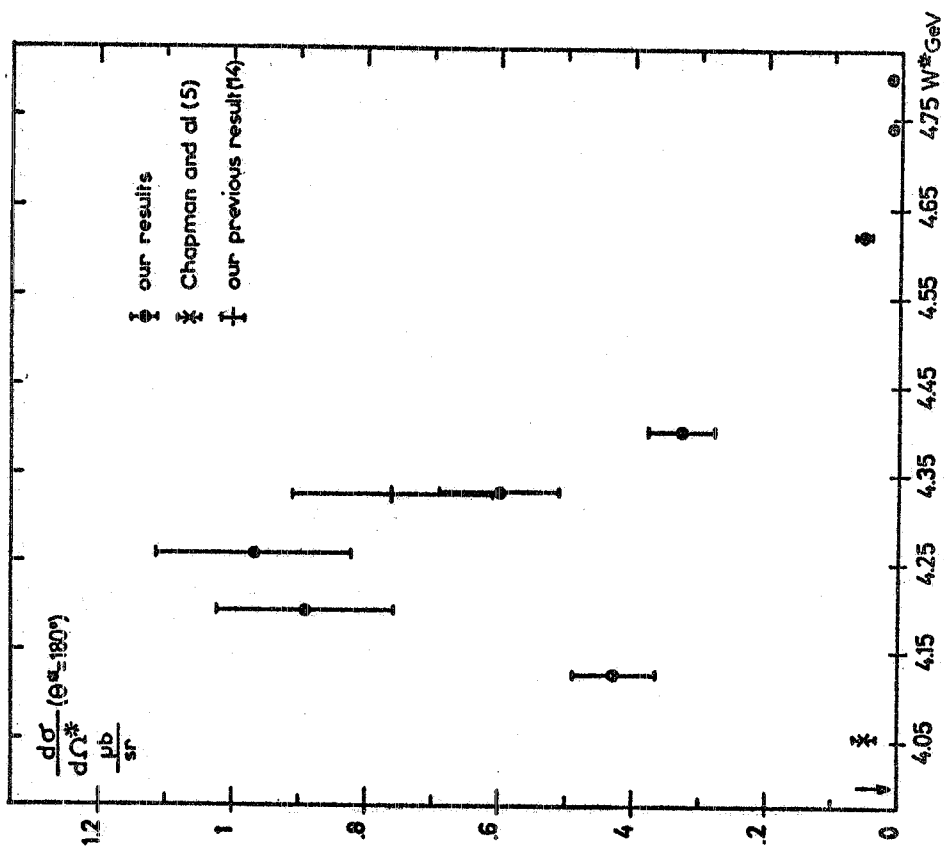


FIG. 19 - Alpha production cross section  $\theta_{\text{c.m.}}^* = 0^\circ$  or  $180^\circ$ , as a function of the energy in the centre of mass. The arrow shows the  $2\pi$  production threshold.

reactions  $d+p \rightarrow \text{He}^3 + X$  and  $d+d \rightarrow \text{He}^4 + X$  as a function of  $W^x - m_3$ , where  $m_3$  is the mass of the detected nucleus  $\text{He}^3$  or  $\text{He}^4$ . From this we can see:

- i) that productions are equal to within 20%;
- ii) that each of these curves has its maximum in the energy region  $W^x$  where the ABC effect is most strongly produced;
- iii) that the production maxima are situated at 570 MeV above the  $d+p \rightarrow \text{He}^3 + X$  threshold, and at only 510 MeV above the  $d+d \rightarrow \text{He}^4 + X$  threshold.

The results obtained at 2.5 GeV/c for different angles, Figs. 9-14, show that the laboratory cross sections decrease as the alpha emission angle is increasing, but that this decrease is much more rapid for the central bump than for the first peak. The total alpha production cross section for deuterons at 2.5 GeV/c deduced from these spectra is  $1.72 \pm 0.5 \mu\text{b}$ . For deuterons at 1.69 GeV/c, Chapman et al found a total cross section of  $0.6 \mu\text{b}$  by assuming, though it is far from being the case at 2.5 GeV/c, that alpha production was isotropic(5).

#### 4.3. - The DEF effect. -

The spectra obtained in this experiment do not have any enhancements directly revealing the DEF effect that was observed around 450 MeV/c in the inclusive reaction  $d+p \rightarrow \text{He}^3 + X$  (13, 7). Nevertheless, a slight production excess in the missing mass region between 400 and 500 MeV/c<sup>2</sup> can be observed on some spectra, in particular those in Figs. 10 and 15, but in the absence of any model that correctly reproduces the ABC effect in this reaction, it is not possible to attribute this production excess either to the ABC effect or to a possible production of the DEF effect. It must however be noticed that contrary to what happens in the ABC effect, the cross sections that could possibly be attributed to the DEF effect are markedly smaller in the reaction studied here (3 or 4 times) than those that were found in the reaction  $d+p \rightarrow \text{He}^3 + X$ .

#### 4.4. - Interpretation. -

The ABC effect has already been the subject of several interpretations, but the authors have never applied their models to the reaction  $d+d \rightarrow \text{He}^4 + X$ . In all the models, the principal parameters given by the authors are connected either to the difficulty of forming nuclei from other lighter nuclei at high energy, or to the influence of intermediate isobar excitation during the reaction. Two simple models illustrate these approaches: Brody takes into account the difficulty of forming an  $\text{He}^3$  in the reaction  $d+p \rightarrow \text{He}^3 + X$  by multiplying the phase space by a factor  $t^{-n}$  (where  $t$  is a 4-momentum-transfer squared)(15), while Dubal and Brown linked the ABC effect to the intermediate production of  $N^x(1470)$ (16). These models

do not give good results for the reaction studied here. In addition, they have little predictive value, and are more a parametrization of the ABC effect using a particular variable; a transfer exponent in<sup>(15)</sup>, or the mass of the intermediate isobar state in<sup>(16)</sup>. More elaborate models that take into account the whole spectrum give interesting results for the reactions for which they were developed. The one pion exchange model with formation of two intermediate  $\Delta$ , Fig. 21a, proposed by Risser and Shuster<sup>(17)</sup>, gives results that are in good agreement with the experiment for the reaction  $n+p \rightarrow d+X$ . The authors have not yet extended the model to the reaction  $d+p \rightarrow \text{He}^3+X$  or to  $d+d \rightarrow \text{He}^4+X$ . Barry, in an article reviewing the ABC effect<sup>(18)</sup>, did apply it to the latter, and found the cross sections much too weak to account for the experimental spectra. In an earlier calculation Anjos et al<sup>(19)</sup> satisfactorily reproduced the results obtained in

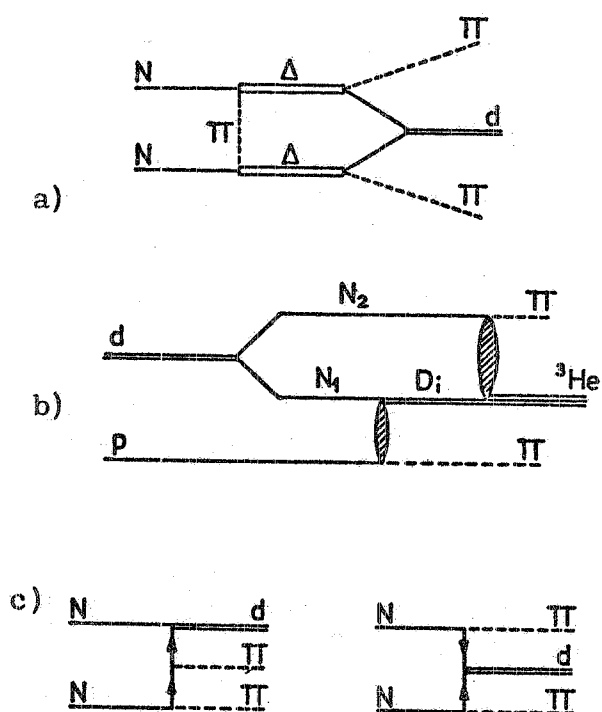


FIG. 21 - Graphs of different models proposed to explain the ABC effect.

the reaction  $d+p \rightarrow \text{He}^3+X$ , using a two-step process which is represented in Fig. 21b. Since this model can not be directly extended to other reactions, the same authors have just published an interpretation of the ABC effect for the reaction  $n+p \rightarrow d+X$ <sup>(19)</sup>, based on a generalisation of the Deck effect, Fig. 21c. Unfortunately their calculation has not been applied to the reaction  $d+d \rightarrow \text{He}^4+X$ . We think, however, that the results obtained here in this reaction provide an excellent means of testing models that describe the ABC effect since alpha production is almost uniquely linked with it, and since the cross sections are nearly as large, and even larger if only the first peak is considered<sup>(20)</sup>, as those obtained in  $d+p \rightarrow \text{He}^3+X$  in analogous kinematic conditions (see Fig. 20).

## 5. - I=0 MESON RESONANCES OF MASS BETWEEN 500 AND 1000 MeV/c<sup>2</sup> .-

The study of I=0 meson resonances in pion-nucleon production experiments is always very difficult, since these experiments require either the detection of neutral particles, as in  $\pi^-+p \rightarrow n+X$ , or else the detection of several charged particles as in  $\pi^++p \rightarrow (\Delta^{++})+X$ , or,  $\pi^++d \rightarrow p+p+X$ . A reaction such as  $d+d \rightarrow \text{He}^4+X$  would then seem well adapted to such a

study, since the missing meson mass is in a pure  $I=0$  state and is associated with only one charged particle. Since alpha has spin  $j=0$ , only positive parity states can be created in the S wave. All  $I=0$  mesons, such as  $\eta^0$ ,  $\omega^0$ ,  $\eta'$  require an odd wave, except for the possible  $\varepsilon^0$  meson ( $I^G, J^P = 0^+, 0^+$ ) which may be created in the S wave.

The  $\varepsilon^0$  resonance expected around 700 to 800 MeV/c<sup>2</sup> in the S wave of  $\pi\pi$  scattering<sup>(21)</sup> has never been convincingly seen in  $2\pi^0$  production experiments such as  $\pi^- + p \rightarrow \pi^0 + \pi^0 + n$  and  $\pi^+ + d \rightarrow p + p + \pi^0 + \pi^0$ , and its observation in the  $\pi^+ \pi^-$  mode is obscured by the production of the  $\rho$  meson.

The other method of looking for it is to use the Chew-Low extrapolation applied to the reactions  $\pi^- + N \rightarrow \pi + \pi + N$  to do a phase shift analysis of the  $\pi\pi$  reaction. After numerous tries with weak statistics, the results obtained using this method now converge towards a unique solution for the S-wave different from that first expected. The resonance found is linked to the inelastic threshold  $\pi\pi \rightarrow K\bar{K}$ , where the S wave phase shift passes through 90° and where the elasticity parameter goes suddenly from 1 to 0.5. The formulation of this result depends much more on the definition given of a resonance than on the experimental results. On this point, it should be noted that the latest results obtained for  $\pi^0 \pi^0$ <sup>(22)</sup>, which are in agreement with the present phase shift analyses, give a large bump at about 800 MeV/c<sup>2</sup>.

The experimental results obtained by counting alphas emitted at  $\theta_{lab} = 0^\circ$  for incident momenta of 3.32, 3.66, and 3.82 GeV/c let us study the mass region of the  $\varepsilon^0$  and of other mesons of mass less than 1000 MeV/c<sup>2</sup>. Results are given in Figs. 16, 17 and 18. On these spectra we can see that:

i) the rate of alpha production is very weak, of the order of a few  $\mu\text{b}/(\text{sr}, \text{GeV}/c)$  which after integration in the centre of mass system gives production cross sections  $d\sigma/d\Omega^*$ ,  $\theta^* = 180$  or  $0^\circ$  respectively equal to  $52.9 \pm 8.2$ ,  $18.9 \pm 2.9$ , and  $20.7 \pm 3.2$  nb/sr;

ii) alpha production associated with missing masses of less than 550 MeV/c<sup>2</sup> disappears with the ABC effect;

iii) the three momentum spectra show a structure situated in the region of 800 MeV/c<sup>2</sup>.

In order to determine the characteristics of this structure, we compared it to a Gaussian superimposed on a continuum represented by a polynomial. In the three cases, the best fit corresponds to a third degree polynomial. The parameters obtained for the Gaussian, and their uncertainties, are given in Table II. The central mass is not very far from 783 MeV/c<sup>2</sup>, the mass of the  $\omega^0$ . We have also simulated the shape of the momentum spectrum that  $\omega^0$  would have in our reaction, taking into account its natural width and the resolution of our apparatus. This calculation showed that the Gaussian-form hypothesis used above was justified, and has led

to the "calculated" parameters shown in Table II. The uncertainties associated with the central momenta are due to experimental errors in the angle and in the incident and analysed momenta. Comparison of fitted results with values calculated for the  $\omega^0$  show that it is reasonable to attribute the observed structures to  $\omega^0$  production. The natural widths observed, although larger than those calculated for the  $\omega^0$ , are however too small to be linked with those observed in  $\pi^0\pi^0$ , which are always greater than  $100 \text{ MeV}/c^2$  (22). The cross sections in the last column of Table II are very small, and do not allow observation of variations with respect to energy. As for the other mesons,  $\eta$ ,  $\eta'$ ,  $\phi$ , our spectra contain no evidence of their production. At  $3.32 \text{ GeV}/c$  (see Fig. 16) if the slight deviation observed in the spectrum around  $550 \text{ MeV}/c^2$  corresponded to the  $\eta$ , then it would give a cross section  $d\sigma/d\Omega^* = 1.4 \pm 0.4 \text{ nb/sr}$ . At  $3.82 \text{ GeV}/c$  (see Fig. 22) we can fix the limit for the  $\eta$  at  $0.7 \text{ nb/sr}$ , and for  $\eta'$  at  $0.08 \text{ nb/sr}$ . These values can be compared to other values obtained in meson production reactions involving the formation of light nuclei, such as  $d+p \rightarrow \text{He}^3 + \eta^0$  where the  $\text{He}^3$  is detected at  $180^\circ$  in the centre of mass. In this reaction, where the exchange of two baryons also occurs, the cross sections found,  $\sim 8 \text{ nb/sr}$  (8), are distinctly larger than the limits found here.

## 6. - CONCLUSIONS. -

We have presented a large study of the inclusive reaction  $d+d \rightarrow \text{He}^4 + X$  as a function of energy and production angles. The most striking feature is the very rapid variation with respect to energy of the inclusive alpha production cross section at  $0^\circ$ , Fig. 19. The ratio of the cross sections obtained with deuterons of  $2.3$  and  $3.8 \text{ GeV}/c$  is of the order of  $50/1$ . This variation is essentially due to the ABC effect which shows up here in the form of very impressive peaks. This effect completely dominates the production of several pions in the region of weak missing masses, to such a degree that there is no production at all at  $3.8 \text{ GeV}/c$ , the point where the effect disappeared. The characteristics obtained for the ABC effect in this reaction are so marked that they provide for it an excellent test for models proposed to explain the effect in its various forms.

As for missing masses greater than  $500 \text{ MeV}/c^2$ , the continuum produced is very weak ( $d\sigma^2/dpd\Omega \sim 1 \mu\text{b}/(\text{sr} \cdot \text{GeV}/c)$ ). We observed no signal for the  $\epsilon^0$ , despite favourable conditions (S wave), or for the  $\eta$ , or the  $\eta'$ . Only a weak signal attributed to the  $\omega^0$  was observed.



TABLE II

Comparison of the characteristics of the structures observed on the spectra with those of the  $\omega^0$ .

| P <sub>1</sub><br>GeV/c | Third degree polynomial fit + gaussian,<br>Gaussian parameters |                    |                            |                                   | "Calculated" parameters for $\omega^0$ |                            |                                   | $\frac{d\sigma}{d\Omega^*} \theta^* = 180^\circ$<br>nb/sr |
|-------------------------|--|--------------------|----------------------------|-----------------------------------|--|----------------------------|-----------------------------------|---|
|                         | Central value  |                    | $\sigma$ gaussian<br>MeV/c | Total width<br>MeV/c <sup>2</sup> | Central value<br>MeV/c                 | $\sigma$ gaussian<br>MeV/c | Total width<br>MeV/c <sup>2</sup> |   |
|                         | MeV/c  | MeV/c <sup>2</sup> |                            |                                   |  |                            |                                   |   |
| 3.32                    | 2228.8 ± 7.9   | 788.0 ± 4.0        | 41.5 ± 9.0                 | 50.8 ± 4.7                        | 2224.2 ± 11.7                          | 23.4                       | 28.6                              | 1.0 ± 0.28  |
| 3.66                    | 2202.4 ± 9.3   | 792.0 ± 7.0        | 43.3 ± 11.4                | 81.2 ± 11.4                       | 2196.3 ± 11.0                          | 20.7                       | 38.7                              | 1.57 ± 0.48   |
| 3.82                    | 2174.3 ± 5.0   | 768.0 ± 4.5        | 28.9 ± 4.1                 | 61.8 ± 4.1                        | 2193.8 ± 11.0                          | 25.7                       | 54.9                              | 1.30 ± 0.28   |

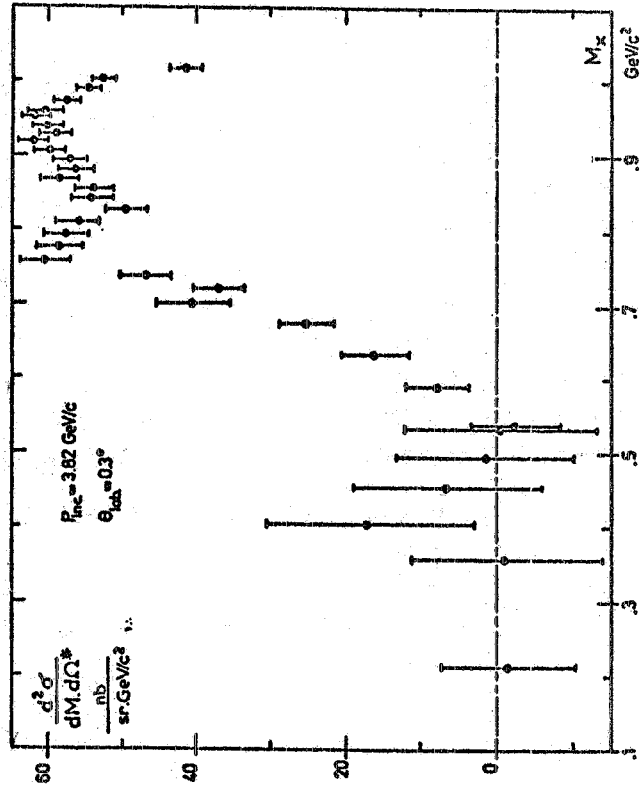


FIG. 22 - Mass spectrum of alphas produced at 0.30 in the laboratory by deuterons at 3.82 GeV/c after transformation in the centre of mass.

We should like to thank the CEA, the  $IN^2P^3$ , and the CNEN of Frascati for making this study possible. In particular we thank the personnel of the synchrotron Saturne for supplying us with an excellent deuteron beam and the Service des Cibles of the DPHPE for producing our deuterium target; we thank also our technicians, P. Guillouet and G. Simoneau for their efficient aid, also Dr. T. Risser for his participation in the initial stages of the experiment, and Dr. F. Lefebvres for his valuable discussions. Finally, we are grateful to Dr. P. Fleury for a determinant discussion on this experiment.

#### REFERENCES. -

- (1) - Y. K. Akimow, O. V. Savchenko and L. M. Soroko, Soviet Physics-JETP 14, 512 (1962); A. Poirier and M. Pripstein, Phys. Rev. 130, 1171 (1963).
- (2) - J. Banaigs, J. Berger, L. Goldzahl, L. Vu Hai, M. Cottureau, C. Le Brun, F. L. Fabbri and P. Picozza, Phys. Letters 53B, 390 (1974).
- (3) - J. Debaisieux, F. Grard, J. Heughebaert, R. Servranckx and R. Windmolders, Nucl. Phys. 70, 603 (1965).
- (4) - A. T. Gøshaw and M. J. Bazin, Phys. Rev. Letters 25, 50 (1970).
- (5) - K. R. Chapman, J. D. Jafar, G. Martelli, T. J. Mac Mahon, H. B. Van Der Raay, D. H. Reading, R. Rubinstein, K. Ruddick, D. G. Ryan, W. Galbraith and P. Sharp, Phys. Letters 21, 465 (1966).
- (6) - J. Banaigs, J. Berger, J. Duflo, L. Goldzahl, M. Cottureau and F. Lefebvres, Proc. of the Topical Seminar on Interactions of Elementary Particles with Nuclei, Trieste (1970), p. 155.
- (7) - J. Banaigs, J. Berger, L. Goldzahl, T. Risser, L. Vu Hai, M. Cottureau and C. Le Brun, Nucl. Phys. B67, 1 (1973).
- (8) - J. Banaigs, J. Berger, L. Goldzahl, T. Risser, L. Vu Hai, M. Cottureau and C. Le Brun, Phys. Letters 45B, 394 (1973).
- (9) - J. P. Meyer, Astron. Astrophys. Suppl. 7, 417 (1972); P. S. Schwaller, B. Favier, D. F. Measday, M. Pepin, P. V. Renberg and C. Serre, Report CERN 72-13 (1972).
- (10) - J. Banaigs, J. Berger, J. Duflo, L. Goldzahl, O. Harff, M. Cottureau, F. Lefebvres, H. Quechon and P. Tardy-Joubert, Nucl. Instr. and Meth. 95, 1479 (1971).
- (11) - A. Abashian, N. E. Booth, K. H. Crowe, R. E. Hill and E. H. Rogers, Phys. Rev. 132, 2296 (1963) (Four articles in sequence).
- (12) - R. J. Homer, O. H. Khan, W. K. McFarlane, J. S. C. Mc Kee, A. W. O'Dell, L. Riddiford, P. G. Williams and D. Griffiths, Phys. Letters 9, 72 (1964); J. H. Hall, T. A. Murray, and L. Riddiford, Nucl. Phys. B12, 573 (1969); G. Bizard, F. Bonthonneau, M. Cottureau, J. L. Laville, C. Le Brun,

- F. Lefebvres, J.C. Malherbe, R. Regimbart, J. Berger, J. Duflo, L. Goldzahl, F. Plouin and L. Vu Hai, Communication to the Conference on High Energy Physics and Nuclear Structure, Uppsala (1973).
- (13) - J. Banaigs, J. Berger, J. Duflo, L. Goldzahl, M. Cottureau and F. Lefebvres, Nucl. Phys. B28, 509 (1971).
- (14) - J. Banaigs, J. Berger, L. Goldzahl, T. Risser, L. Vu Hai, M. Cottureau C. Le Brun, F.L. Fabbri and P. Picozza, Phys. Letters 43B, 535 (1973).
- (15) - H. Brody, Phys. Rev. Letters 28, 1217 (1972).
- (16) - L. Dubal and D.J. Brown, Nucl. Phys. B32, 535 (1973).
- (17) - T. Risser and M.D. Shuster, Phys. Letters 43B, 68 (1973); I. Bar Nir, T. Risser, M.D. Shuster, Nucl. Phys. B87, 109 (1975).
- (18) - G.W. Barry, Nucl. Phys. B85, 239 (1975).
- (19) - J.C. Anjos, D. Levy and A. Santoro, Nucl. Phys. B67, 37 (1973); Saclay-Preprint D.Ph. T/75-5 (1975).
- (20) - J. Banaigs, J. Berger, M. Cottureau, F.L. Fabbri, L. Goldzahl, C. Le Brun, P. Picozza and L. Vu Hai, Frascati Report LNF-74/71(P) (1974), and Proc. of the Topical Meeting on High Energy Collisions involving Nuclei, Trieste (1974).
- (21) - J. P. Baton and J. Regnier, Nuovo Cimento 36, 1149 (1965).
- (22) - W.D. Apel, J.S. Auslander, H. Muller, G. Sigurdsson, H.M. Staudenmaier, U. Stier, E. Bertolucci, I. Mannelli, G. Pierazzini, P. Rehak, A. Scribano, F. Sergiampietri and M.L. Vincelli, Phys. Letters 41B, 542 (1972); K. J. Braun and D.B. Cline, Phys. Rev. D8, 3794 (1973); A. Skuja, M.A. Wahlig, T.B. Risser, M. Pripstein, J.E. Nelson, I.R. Linscott, R.W. Kenney, O.I. Dahl and R.B. Chaffee, Phys. Rev. Letters 31, 653 (1973); G. Villet, M. David, R. Ayed, P. Bareyre, P. Borgeaud, J. Erwein, J. Feltesse, Y. Lemoine, P. Marty and A.V. Stirling, Contribution n° 310 to the II<sup>nd</sup> Intern. Conf. on Elementary Particles, Aix en Provence (1973).